Am J Transl Res 2024;16(8):3922-3937
www.ajtr.org /ISSN:1943-8141/AJTR0154371

Original Article

The Cdc42/Rac1 pathway: a molecular mechanism behind iron-deficiency-driven aortic medial degeneration

Su Wang[1*], Hengjuan Liu[1*], Junxia Hu[2], Ting Li[3], Bowen Li[2]

[1]*Department of Anesthesiology, Renmin Hospital of Wuhan University, Wuhan 430060, Hubei, China;*
[2]*Department of Cardiovascular Surgery, Renmin Hospital of Wuhan University, Wuhan 430060, Hubei, China;*
[3]*Department of Skin Medical Cosmetology, Renmin Hospital of Wuhan University, Wuhan 430060, Hubei, China.*
[*]*Equal contributors.*

Received November 12, 2023; Accepted July 3, 2024; Epub August 15, 2024; Published August 30, 2024

Abstract: Objective: To elucidate the underlying mechanism of iron deficiency augmented Angiotensin II-induced aortic medial degeneration. Methods: ApoE$^{-/-}$ mice were randomly divided into four groups: normal control group (NC group), Angiotensin II (Ang II) subcutaneous pumped alone Group (Ang II group), iron deficiency (ID) group (ID group) and ID+Ang II group. The survival time, systolic blood pressure (SBP), and aortic medial degeneration (AMD) formation were monitored. Iron deposition in the aortas was assessed using Prussian blue iron staining. The expression of iron metabolism indicators, aortopathies and the cytoskeleton of vascular smooth muscle cells (VSMCs) were analyzed. In an in vitro setting, deferoxamine (DFO) was employed to mimic ID to examine the effects of Ang II on the cytoskeletal and contractile function of VSMCs during ID. Ras-related C3 botulinum toxin substrate 1 (Rac-1) expression was inhibited with EHT1864 to verify the role of Cdc42/Rac1 pathway in this pathological process. Blood samples were collected from 150 patients with aortic dissection (AD) and 60 patients with hypertension who were admitted to the Department of Cardiovascular Surgery at Renmin Hospital of Wuhan University between June 2018 and September 2019. The aortic tissues were obtained during the surgical treatment of Stanford type A AD patients and the heart donor. The iron metabolism status in plasma and aortic tissue was analyzed. Results: In vivo experiments revealed that, in comparison to the NC and ID groups, mice in the Ang II and ID+Ang II groups exhibited increased SBP, significantly reduced survival time, and an expanded range of aortic dissection ($P < 0.05$). ID feeding augmented the Ang II-induced aortopathies. Both in vitro and in vivo results indicated that ID led to diminished expression of phosphorylated myosin light chain (p-MLC) and recombinant Cell Division Cycle Protein 42 (Cdc42) in VSMCs, while Rac-1 expression increased. The clinical sample testing data further confirmed the discovery that individuals diagnosed with AD display ID in both the plasma and the diseased aortas. Conclusions: The Cdc42/Rac1 pathway plays a crucial role in disrupting the cytoskeleton of vascular smooth muscle cells during iron deficiency, which leads to aortic medial degeneration both in vivo and in vitro.

Keywords: VSMCs, iron deficiency, aortic medial degeneration, aortic dissection

Introduction

Aortic dissection (AD) is a serious cardiovascular emergency with rapid progression and high early mortality. Epidemiological studies have shown that the incidence of aortic dissection (AD) in hypertensive patients is increasing year by year, which brings serious hidden danger and burden to families and society [1, 2]. Aortic medial degeneration (AMD) is the primary pathological feature of AD [3], yet the pathogenesis of AMD has not been fully explored. Previous research has shown that dysfunction of vascular smooth muscle cells (VSMCs) contributes to AMD formation, but the primary underlying factors require further elucidation [4]. Disturbed trace element metabolism leads to cellular dysfunction and promotes tissue damage [5, 6]. Therefore, maintaining trace element homeostasis in hypertensive patients is a potential preventive strategy against AMD.

Iron is the most abundant element in the human body, and disorders of iron metabolism are

https://doi.org/10.62347/YISX1726

widespread [7]. Cells must maintain a sufficient iron supply for essential physiological and developmental processes [8], while simultaneously regulating the labile iron pool to prevent excessive generation of reactive oxygen species through the Fenton reaction [9]. Research has shown that iron deficiency (ID) plays a significant role in the development of cardiovascular disease [10]. ID impacts cardiac function by diminishing cell motility and curtailing oxidative phosphorylation in cardiomyocytes [11]. In the context of chronic heart failure, clinical outcomes are worse in non-anemic iron-deficient patients compared to those who are anemic and iron deficient [12]. This observation suggests that ID might directly impact cardiomyocytes, independent of the presence of anemia [13]. The correlation between iron metabolic status and the occurrence of AMD remains controversial. It has been reported that iron overload contributes to aortic wall erosion and the incidence of aortic aneurysm by amplifying oxidative stress within the aortic walls and promoting macrophage infiltration [14, 15]. Similarly, two other large studies observed a reduction in iron ion and transferrin receptor 1 (TFR1) levels in the circulation of patients with abdominal aortic aneurysms [16, 17]. In addition, serum iron ion concentrations were significantly elevated in patients with thoracic AD; however, it remained unaltered within the aortic tissue [18]. While these studies have focused on investigating whether iron metabolism disorders play a role in the progression of AMD, the precise underlying mechanisms by which abnormal iron metabolism contributes to the development of AMD remain elusive. Our initial experiments revealed a reduction of iron content in both circulating blood and aortic mesothelium among AD patients [18]. Here, we investigate the effect of ID on Angiotensin II (Ang II)-induced AMD and the possible underlying mechanism.

Materials and methods

Mice and modeling

10-week-old male ApoE$^{-/-}$ mice, weighing 20-22 g, were utilized in the Cardiovascular Surgery Laboratory, Renmin Hospital of Wuhan University. Subcutaneous infusion of Ang II (Alzet, model #2004; 1 μg/kg/min) for 4 weeks was used as an AMD model [4]. An ID model was generated through the administration of a low-iron diet (5 ppm iron/kg diet). The combination of Ang II administration and a low-iron diet in ApoE$^{-/-}$ mice is employed to simulate a condition of hypertension accompanied by iron deficiency (ID+Ang II). The control group was provided with a normal-iron control (NC) diet. At the end of the experiment (T4 weeks), the mice were humanely euthanized by decapitation under 4% isoflurane anesthesia, and the aortic tissues were harvested. All experimental procedures followed the National Institutes of Health Guide for the Care and Use of Laboratory Animals and were permitted by the Laboratory Animal Welfare & Ethics Committee (IACUC) of Wuhan University (WDRM-20201107).

Iron intervention and cellular function experimental study in vitro

Human aortic vascular smooth muscle cells (HASMCs) were purchased from ATCC and cultured in Dulbecco's Modified Eagle Medium (DMEM) supplemented with 10% fetal bovine serum, 1% penicillin, 2 mM glutamine, and 50 μg/mL each of gentamicin and amphotericin B. Cells were incubated at 37°C in an atmosphere containing 5% CO_2. Iron-deficient conditions were established using desferoxamine (DFO), and EHT1864 (Rac1 inhibitor) suppressed Rac1 expression. Cells were treated with 0.1 μM Ang II as described [4], to investigate the effect of ID on both cytoskeletal and functional alterations.

Clinical information collection

All experimental procedures involving human specimens were formulated in compliance with the Declaration of Helsinki and received approval from the Ethics Committee of Renmin Hospital of Wuhan University (WDRY2015K-C022). Furthermore, the trial has been registered with the China Clinical Trials Registry (ChiCTR1800018970). All subjects were informed of the purpose of the trial and signed written informed consent.

Clinical information, blood samples, and aortic tissue specimens were systematically obtained from a total of 150 patients diagnosed with AD and 60 patients diagnosed with hypertension. These patients were admitted to the Department of Cardiovascular Surgery at Renmin Hospital of Wuhan University between June 2018

Table 1. Characteristics of clinical data of patients with aortic dissection and hypertension

Indicators	AD group (n = 150)	Control group (n = 60)	*P* value
Age (year)	55.28 ± 13.28	52.74 ± 11.89	0.0807
Male/Female (n)	110/40	29/31	< 0.0001***
Body mass index	27.86 ± 4.018	21.31 ± 2.778	< 0.0001***
Systolic blood pressure (mmHg)	162.6 ± 2.224	145.2 ± 2.145	< 0.0001***
Smoking history (n)	126	43	0.0638
< 10 cigarettes/day (n)	16	7	0.4714
10-20 cigarettes/day (n)	86	27	0.5687
> 20 cigarettes/day (n)	24	6	1.0000
History of drug exposure (n)	0	0	1.0000
Family history of aortic disease (n)	0	0	0.7525
LVEF (%)	58.14 ± 3.211	57.25 ± 4.358	0.1562
Ultrasound detectable liver injury (n)	132	7	< 0.0001***
Ultrasound detectable renal injury (n)	36	15	0.7420
Comorbidities (n)			
Hypertension	138	60	0.0031**
Diabetes mellitus	18	19	< 0.0001***
Gastrointestinal disorders	15	7	0.4516
Neurodegenerative disease	0	0	1.0000
Type of aortic coarctation (n)	150	0	< 0.0001***
Stanford Type A	66	0	
Stanford Type B	84	0	

Data are expressed as mean ± standard deviation or number of cases. Abbreviations: AD, aortic dissection; LVEF, left ventricular ejection fraction. **P < 0.01, ***P < 0.001 versus control group.

and September 2019. Exclusion criteria encompassed patients demonstrating clinically unstable vital signs, a history of aortic diseases associated with infection, aortitis, or trauma, contraindications to computed tomography angiography (CTA), or incapacity to provide informed consent. Detailed demographic and clinical characteristics of both AD and hypertension are shown in **Table 1**.

Detection of iron metabolism in the serum

A 5 mL blood sample was promptly collected for the purpose of iron metabolism analysis immediately after the patient was admitted to the hospital. The blood sample underwent centrifugation at 2,500 g for 10 minutes at room temperature within 1 hour of collection. Subsequently, the serum was extracted and stored at -80°C. Serum iron levels were quantified by a serum iron detection kit (Nanjing Jiancheng Bioengineering Institute, China). Enzyme-linked immunosorbent assay (ELISA) was used to analyze transferrin (TF) and soluble transferrin receptor (sTFR) levels. The inter-assay and intra-assay coefficients of variation were both below 7% for all data encompassed by the analyses.

Prussian blue iron staining

Tissue specimens from the corresponding segments of the ascending aorta were collected from 15 patients diagnosed with Stanford type A AD who underwent ascending aortic replacement and organ donors with hypertension only, respectively (n = 15). Referring to the method provided in the previous study [19], the specimens were fixed in 4% paraformaldehyde for 24 hours, subsequently subjected to dehydration and embedding. Sections, measuring 4 μm in thickness, were subsequently subjected to dewaxing and hydration procedures, followed by incubation with a 50 μL dilute hydrochloric acid/potassium ferrocyanide solution for a period of 15-20 minutes at room temperature. The samples were further subjected to staining utilizing nuclear fast red solution for a duration of 15-30 seconds. Following nuclear staining with hematoxylin, the sections under-

went dehydration using gradient alcohol and xylene. Images were captured with the optical microscope (OLYMPUS, BX53).

Immunohistochemistry (IHC) staining

Sections underwent the processes of dewaxing, hydration, and immersion in an endogenous peroxidase blocking buffer. Following overnight incubation with about 50 μL of rabbit/mouse primary antibody at 4°C, slides were subjected to incubation with 50 μL of anti-rabbit/mouse IgG at 37°C for 1 hour and subsequently visualized using 3,3'-diaminobenzidine (DAB). Ultimately, the sections were dehydrated and mounted before capturing images using a microscope. Histochemical staining was evaluated according to the previously described methodology [20].

Elastic van Gieson (EVG) staining

After dewaxing and hydration, sections were stained with Verhoeff's hematoxylin solution for 30 minutes at room temperature. Subsequently, they were differentiated using a 2% ferric chloride solution until black fibers and gray backgrounds became visible under the microscope. The samples were diluted using a 5% sodium thiosulfate solution for 1 minute to eliminate iodine, and then restained using Van Gieson solution for 5 minutes. Subsequent to dehydration and transparent treatment with dimethylbenzene, the sections were observed under a light microscope (OLYMPUS, BX53). Black areas correspond to elastic fibers, while red areas represent collagen.

F-actin staining

After dewaxing and hydration, sections of aortic tissue were stained with iFluor488 phalloidin stain for 60 minutes at room temperature, and nuclei were stained with DAPI for 10 minutes in the dark. Images were obtained by a microscope.

Western blot

Total protein was extracted from VSMCs. Equal quantities of protein (10 μg) were separated using sodium dodecyl sulfate-polyacrylamide gel electrophoresis and then transferred onto polyvinylidene fluoride (PVDF) membranes. The membranes were blocked using 5% skimmed milk for 1 hour at room temperature, followed by an overnight incubation with primary antibodies at 4°C. The primary antibodies were labeled as follows: TFR1 (abcam, 1:1000, ab84036), TF (proteintech, 1:1000, 17435-1-AP), Rac-1 (abcam, 1:1000, ab129758), Cdc42 (abcam, 1:1000, ab64533), p-MLC (abcam, 1:1000, ab2480), a-tubulin (proteintech, 1:5000, 11224-1-AP). After incubation with the secondary antibody (LICOR, 1:10,000) for 1 hour at room temperature, the membranes were visualized using an Odyssey CLx.

Statistical analysis

The experimental data were presented as mean ± standard deviation (SD). Student's t-test or non-parametric equivalent was employed for the comparison of data between two groups, the Chi-square or Fisher's exact test was used for categorical variables, and comparisons between three and more groups were assessed by one-way analysis of variance (ANOVA) and Tukey's post-test. The disparities between the survival curves were assessed utilizing the Log-rank test. $^{*}P < 0.05$, $^{**}P < 0.01$ and $^{***}P < 0.001$ indicate statistically significant differences. All the above statistical analyses were performed using the GraphPad Prism 6 software (GraphPad Software Inc., USA).

Results

The co-administration of low iron feeding with Ang II-pumping synergistically augmented AMD formation in mice

To investigate the effect of ID on Ang II-induced AMD formation, ApoE$^{-/-}$ mice were fed a low-iron diet containing 5 ppm of iron, and AMD was induced through subcutaneous Ang II infusion. The survival time of the ID co-administration with Ang II group was significantly shorter than that of the Ang II group. Additionally, the ID+Ang II mice exhibited a more extensive intimal tear. However, ID alone did not affect survival time or systolic blood pressure compared to the control group (**Figure 1A-C**). Prussian blue staining and immunohistochemistry (IHC) showed that ID feeding decreased iron content in the aortic wall (**Figure 1D**, **1E**), accompanied by decreased TF and increased TFR1 expression (**Figure 1F-I**). These results suggest that ID does not affect blood pressure but increases the incidence and severity of Ang II-induced AMD.

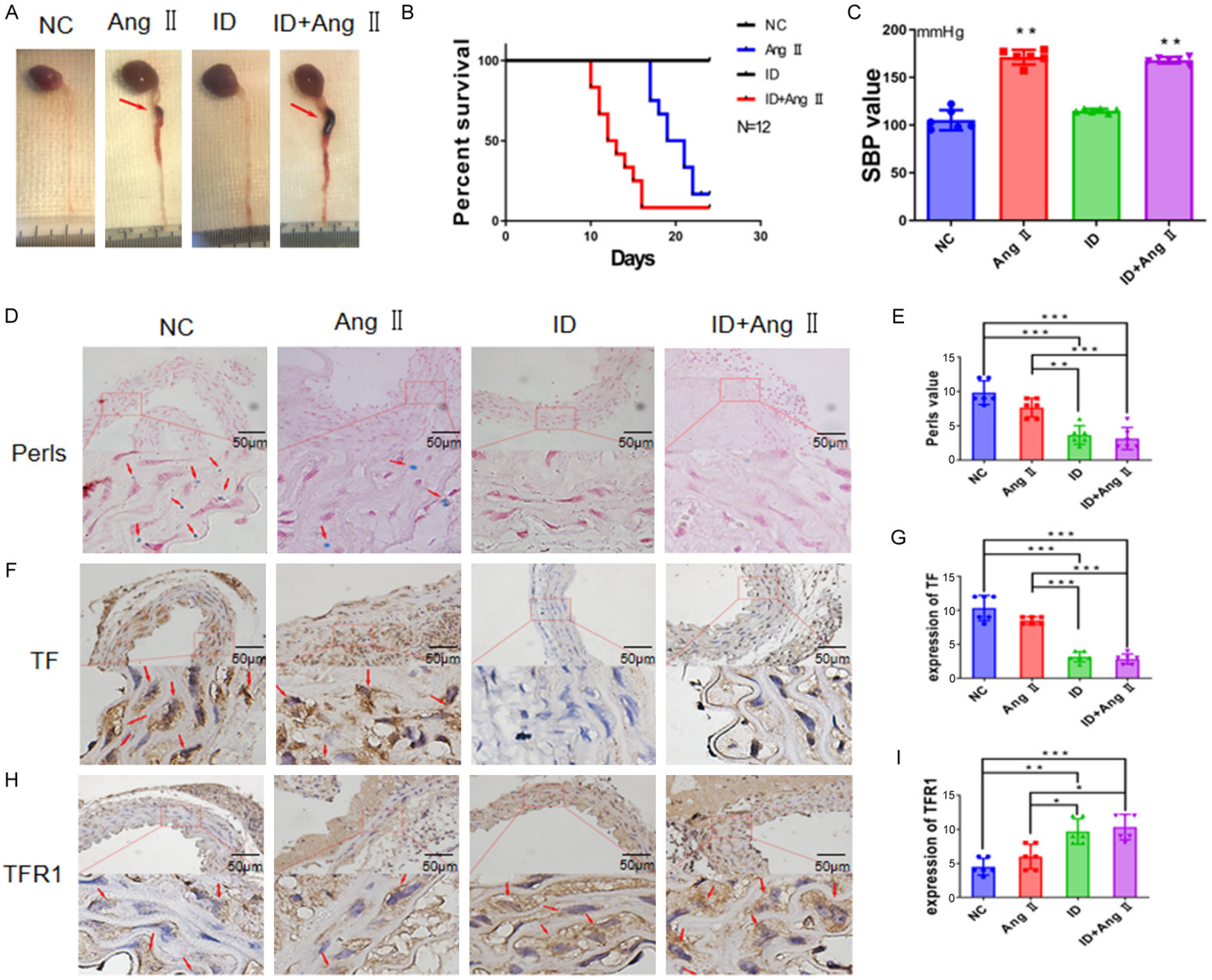
A
NC
Ang Ⅱ
ID
ID+Ang Ⅱ
B
Percent survival
Days
NC
Ang Ⅱ
ID
ID+Ang Ⅱ
N=12
C
SBP value
mmHg
D
Perls
E
Perls value
F
TF
G
expression of TF
H
TFR1
I
expression of TFR1
50μm

Figure 1. ID increased both the incidence and severity of Ang II induced AMD in mice. The extent of tearing in AD was heightened in mice with ID combined with Ang II induction (A). The survival time of the ID combined with Ang II group was significantly shorter than that of the Ang II group (B). ID alone did not affect survival time or systolic blood pressure compared with the control group (B, C). ID feeding resulted in a decrease in iron content within the aortic wall (D, E), accompanied by decreased TF and increased TFR1 expression (F-I). Values are presented as the mean ± SD. The statistical analyses between multiple groups were performed by one-way ANOVA and Tukey's post-test. $*P < 0.05$, $**P < 0.01$, $***P < 0.001$. AD, aortic dissection; TF, transferrin.

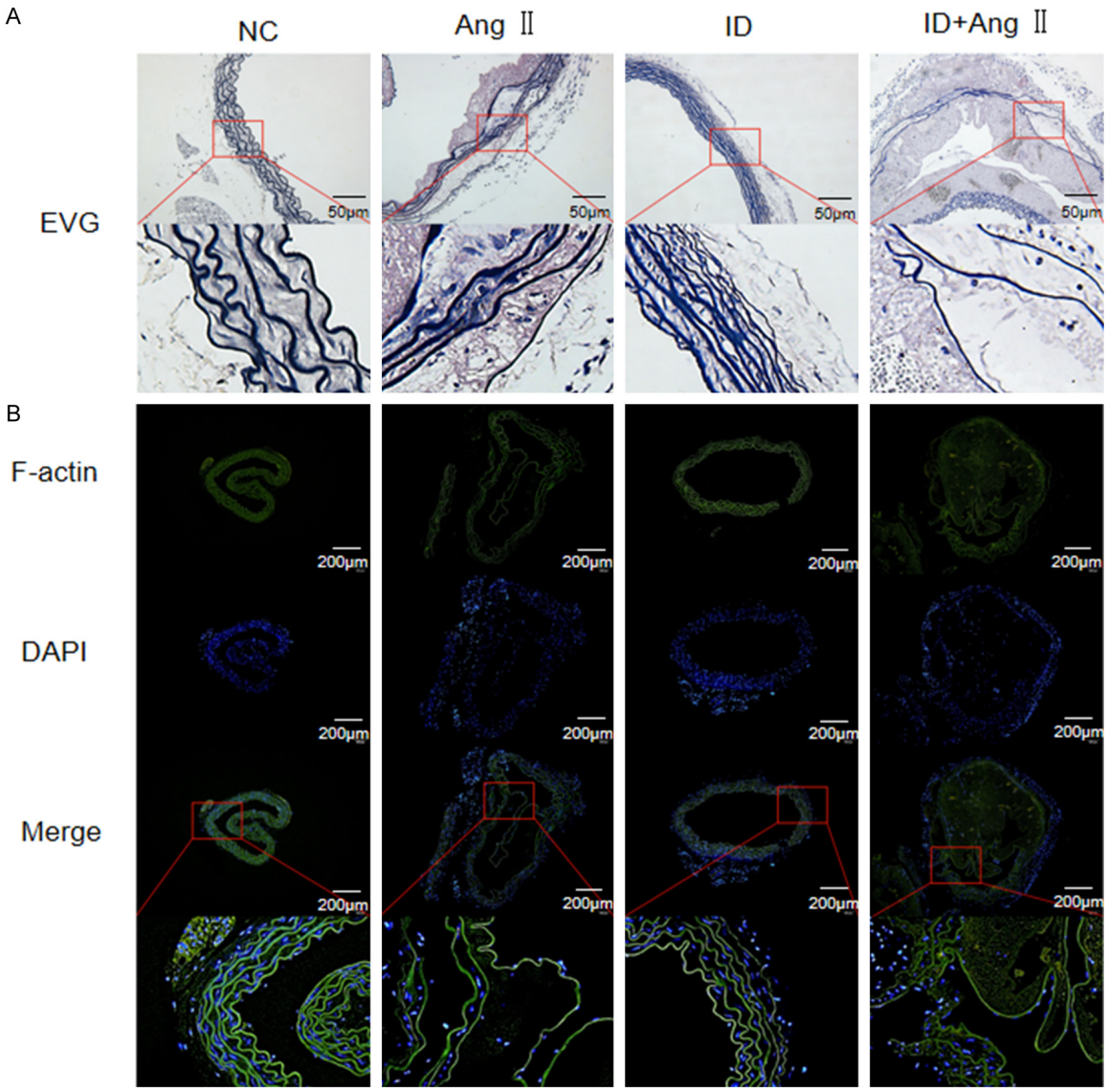

Figure 2. Aortic wall structural alterations in the AMD mice model. In the aortic tissue of AMD mice, the elastic fibers disintegrated and ruptured, while collagen deposition increased in the aortas of mice affected by combined ID and Ang II induction (A). The content of F-actin decreased in the aortas of mice affected by combined ID and Ang II induction (B). AMD, aortic medial degeneration.

ID induced dysfunction and cytoskeletal disruption in aortic VSMCs of mice

Aortic tissues from AMD mice exhibited disintegration and disruption of elastic fibers (black), coupled with increased collagen deposition (red) and reduced F-actin content (**Figure 2A**, **2B**). In addition, IHC analysis revealed that the expression of p-MLC and Cdc42 proteins was significantly decreased in the aortas of ID mice

(**Figure 3A-D**), while Rac1 expression was increased (**Figure 3E**, **3F**). These findings collectively suggest that ID can exacerbate AMD lesions, which may be related to cytoskeletal and VSMC dysfunctional.

ID induced cytoskeletal disruption and dysfunction of VSMCs in vitro

Animal experiments have confirmed that ID regulates the expression of cytoskeletal proteins in VSMCs, but these changes are influenced by multiple factors in vivo. To accurately investigate the effects of ID on the skeletal structure and contractile function of VSMCs, we conducted cellular experiments in vitro. Upon exposure to ID conditions, VSMCs exhibited swelling, reduced expression of F-actin, and increased intercellular gaps when under ID. Moreover, F-actin expression was decreased, with myofilaments displaying unevenly distributed and aggregation towards the cell periphery. While compared to the ID group alone, the expression of F-actin is higher in the ID+Ang II group. Consistent with the study [21], in VSMCs treated with Ang II, F-actin expression was significantly increased with a changed shape of the cell and more lamellipodia formation. (**Figure 4A**, **4B**). What's more, ID further led to a decrease in TF, p-MLC, and Cdc42 protein expression, while TFR1 and Rac1 expression were upregulated (**Figure 5A-D**). These data indicate that ID disrupts the cytoskeleton and contractile function of VSMCs.

ID affects Ang II-induced cytoskeletal disruption and dysfunction of VSMCs in vitro through the Cdc42/Rac1 signaling pathway

To provide deeper insights into the potential mechanisms through which iron deficiency induces cytoskeletal disruption and dysfunction in VSMCs, we used EHT1864 to suppress Rac1 expression in vitro experiments. After use of EHT1864, TFR1 and Rac1 expression was decreased, while the expression of TF, p-MLC and Cdc42 was increased (**Figure 6A-F**). Our results indicate that the application of EHT1864 effectively reversed Ang II-induced cytoskeletal disruption and adjusted iron metabolism dysregulation, and these observations underscore the potential contribution of iron deficiency to the advancement of AMD through the regulation of the Cdc42/Rac1 signaling pathway.

Patient characteristics

Patient characteristics were collected from 150 AD patients and 60 hypertensive patients admitted to the Department of Cardiovascular Surgery, Renmin Hospital of Wuhan University from June 2018 to September 2019. Patients with clinically unstable vital signs, hereditary or traumatic aortic diseases, contraindications to CTA, or those unable to provide informed consent were excluded. The baseline characteristics of the AD and control groups are presented in **Table 1**. There were no significant differences in age, smoking history, and left ventricular ejection fraction between the two groups. However, AD patients exhibited elevated systolic blood pressure, body mass index, and a higher proportion of ultrasound-detected liver damage, while demonstrating a lower prevalence of diabetes.

Iron deficiency but not anemia in circulating of AD patients

In this study, blood samples were collected from 210 patients for analysis of iron metabolism. The iron metabolism indicators are depicted in **Figure 7**. The results of iron metabolism indexes indicated that serum iron ion concentration (Fe^{3+}), total iron binding capacity (TIBC), transferrin saturation (TS) and TF were significantly lower in AD patients compared with control patients (**Figure 7A-D**). There was no significant difference in soluble transferrin receptor (sTFR), while serum ferritin levels were notably elevated in AD patients compared to hypertensive patients (**Figure 7E**, **7F**). Serum concentrations of D-dimer and C-reactive protein (CRP) were higher in AD patients than in hypertensive patients (**Figure 7G**, **7H**). Despite the presence of iron deficiency, there was no significant difference in hemoglobin (Hb) concentration among the groups (**Figure 7I**). Taken together, these data suggest that AD patients present with circulating iron deficiency but not anemia.

AD specimens showed iron deficiency in the middle layer of aorta

Iron deposition in the middle layer of aorta was visualized by Prussian blue staining, which revealed significantly lower iron deposition in the middle layer of the AD aorta compared to the control group (**Figure 8A**, **8B**). Additionally, the expression of iron metabolism-related pro-

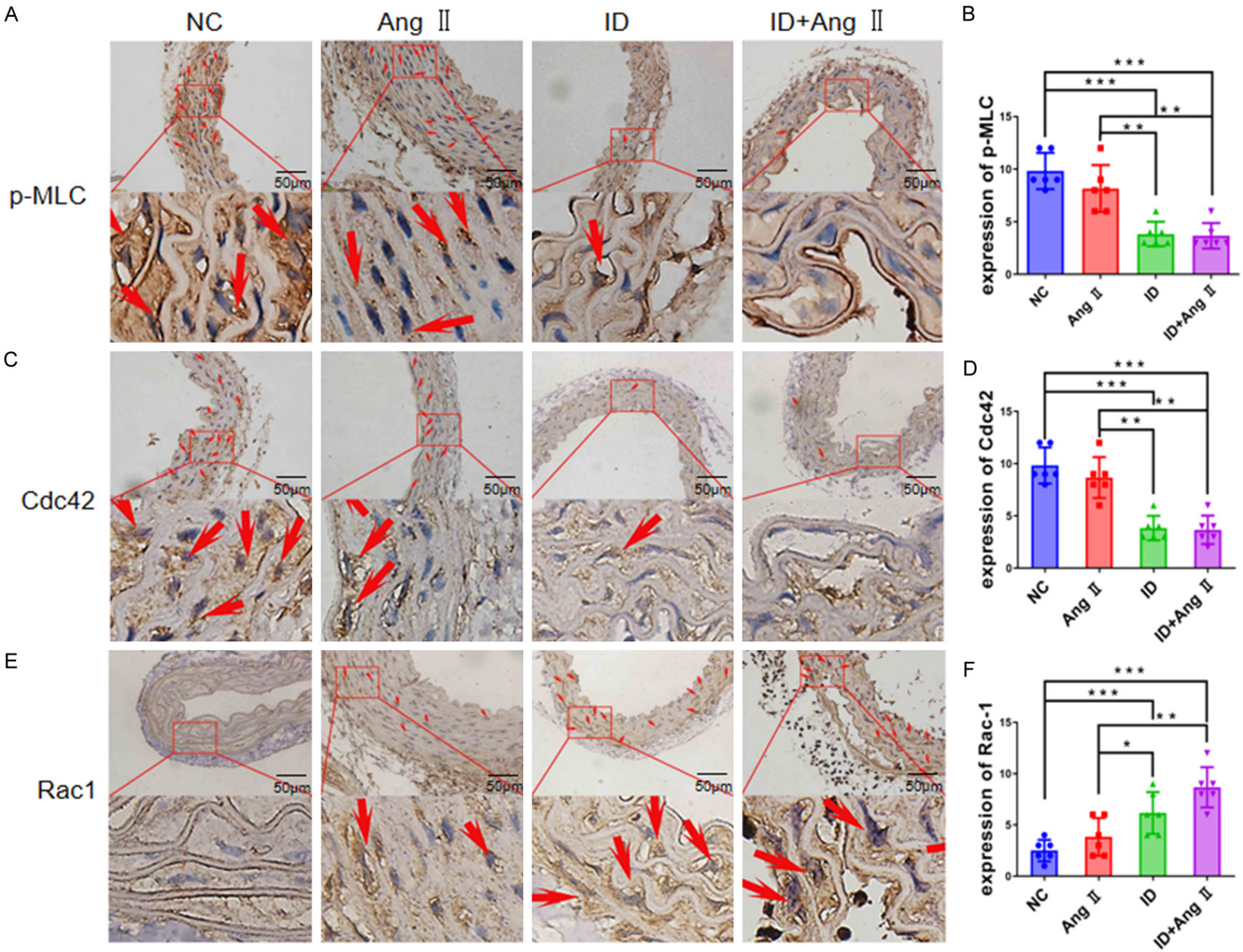
A
NC
Ang Ⅱ
ID
ID+Ang Ⅱ
p-MLC
Cdc42
Rac1
50μm
B
C
D
E
F
expression of p-MLC
expression of Cdc42
expression of Rac-1
NC
Ang Ⅱ
ID
ID+Ang Ⅱ

Figure 3. Alterations in the expression of functional and cytoskeletal proteins in aortic VSMCs in the AMD mice model. IHC indicated that the expression of p-MLC and Cdc42 proteins were significantly decreased in the aortas of mice with ID (A-D), while Rac1 expression increased (E, F). Values are presented as the mean ± SD. The statistical analyses between multiple groups were performed by one-way ANOVA and Tukey's post-test. **P* < 0.05, ***P* < 0.01, ****P* < 0.001. AMD, aortic medial degeneration.

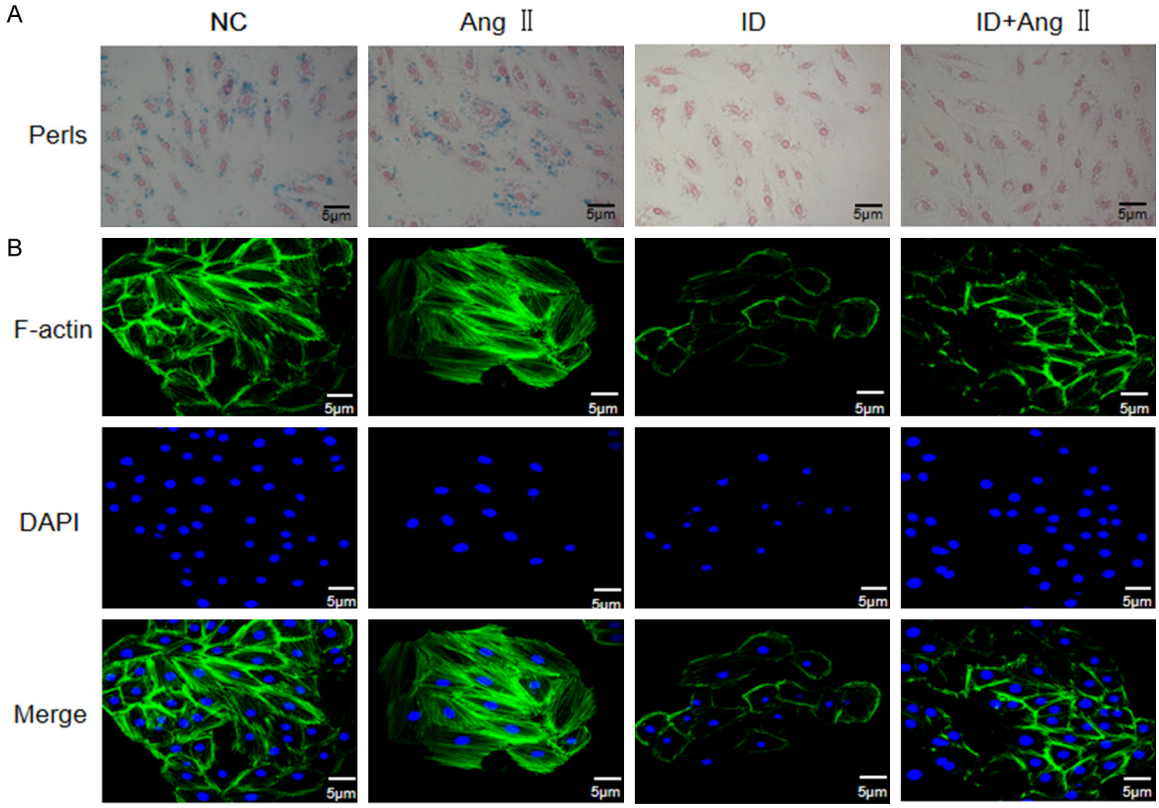

Figure 4. The effects of ID on the skeletal structure of VSMCs in vitro. Iron deficiency led to the swelling of VSMCs, accompanied by a reduction in cell connections (A). Additionally, iron deficiency resulted in decreased expression of F-actin, uneven distribution of myofilaments, and their aggregation towards the cell periphery (B). VSMCs, vascular smooth muscle cells; TFR1, transferrin receptor 1.

teins was assessed using IHC. IHC demonstrated downregulation of TF and upregulation of TFR1 in AD specimens (**Figure 8A**, **8B**). EVG staining revealed increased disintegration and rupture of elastic fibers (black) and deposition of collagen (red) in AD specimens (**Figure 8C**). Furthermore, the expression of F-actin (**Figure 8D**) and p-MLC (**Figure 8A**, **8B**) was significantly decreased in AD tissue compared with normal aortic specimens. Taken together, these results suggest an iron-deficient state in AD specimens, accompanied by irregular aortic mesenchymal matrix and VSMC dysfunction.

Discussion

This study revealed a significant correlation between the presence of iron deficiency (ID) in circulation and the mesangial regions of the aorta. The study also found that vascular smooth muscle cells (VSMCs) dysfunction and cytoskeleton instability of the aortic wall can exacerbate the occurrence and severity of aortic medial degeneration (AMD), leading to disruption of VSMCs regulation in hypertensive patients and mice. Our study suggests for the first time that the Cdc42/Rac1 signaling pathway may be involved in ID and aggravates the progression of AMD. Aortic dissection (AD) is characterized by AMD as its primary pathological feature, which can result in various complications, including life-threatening aortic rupture [22]. Currently, there are no effective pharmaceutical interventions available for the treatment of AD [23]. Therefore, it is crucial to iden-

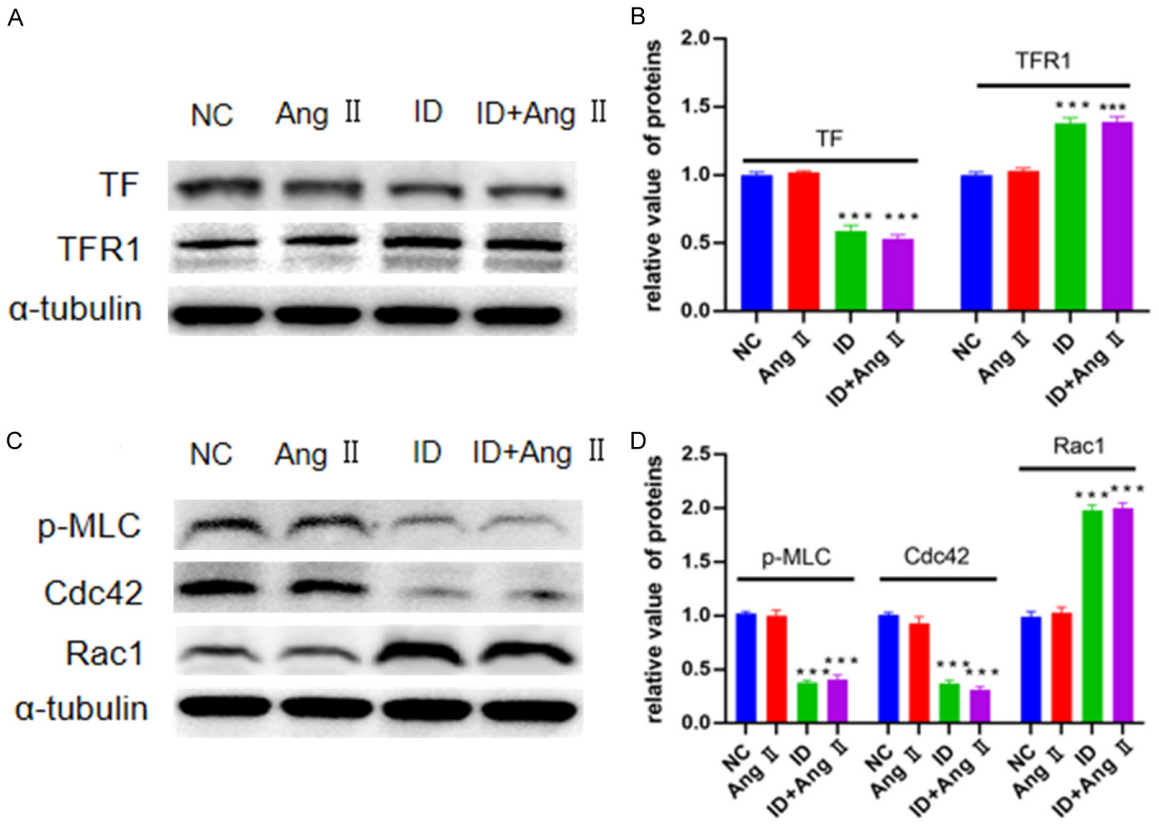

Figure 5. The effects of ID on the contractile function of VSMCs in vitro. In the context of iron deficiency, the expression of TF, p-MLC, and Cdc42 was reduced, while that of TFR1 and Rac1 was increased (A-D). Values are presented as the mean ± SD. ***P < 0.001. VSMCs, vascular smooth muscle cells; TF, transferrin; TFR1, transferrin receptor 1; p-MLC, phosphorylated myosin light chain.

tify the risk factors and underlying mechanisms that contribute to this aortopathy.

Hypertension stands as an independent risk factor for AD prognosis and is associated with notable alterations in the mechanical attributes of the aortic wall, including increased strain-related susceptibility to AD [2, 24-26]. Our previous study found that almost all AD patients had hypertension [18]. In the present study, we specifically enlisted patients with only hypertension to provide a disease-matched control group to investigate why not all hypertensive patients present with AD. Our in vivo results showed that mice subjected to a low-iron diet did not display significant differences in blood pressure compared to the normal diet group in the absence of Angiotensin II (Ang II) intervention. However, administration of Ang II resulted in a significant increase in blood pressure. Interestingly, the survival time of the low-iron group combined with Ang II was significantly shorter, accompanied by a more extensive tear and higher incidence of AD, in contrast to the Ang II group alone. Immunohistochemistry (IHC) analysis further revealed that ID led to a reduction in TF expression and an increase in TFR1 expression. These findings suggest that ID does not exert an influence on blood pressure in mice. However, it amplifies the occurrence and severity of AMD, and ID promotes the formation of AD in hypertensive mice by perturbing the structure of the vessel wall. Moreover, the combination of low iron feeding and Ang II induction exhibits a synergistic effect on the development of AMD in mice.

Previous studies have demonstrated that maintaining the normal cytoskeleton of VSMCs is fundamental for the preservation of cellular function and arterial wall stability [27-30]. Dysfunction of VSMCs constitutes a primary pathological feature of AMD [31-33]. The cytoskeleton has the crucial roles of providing

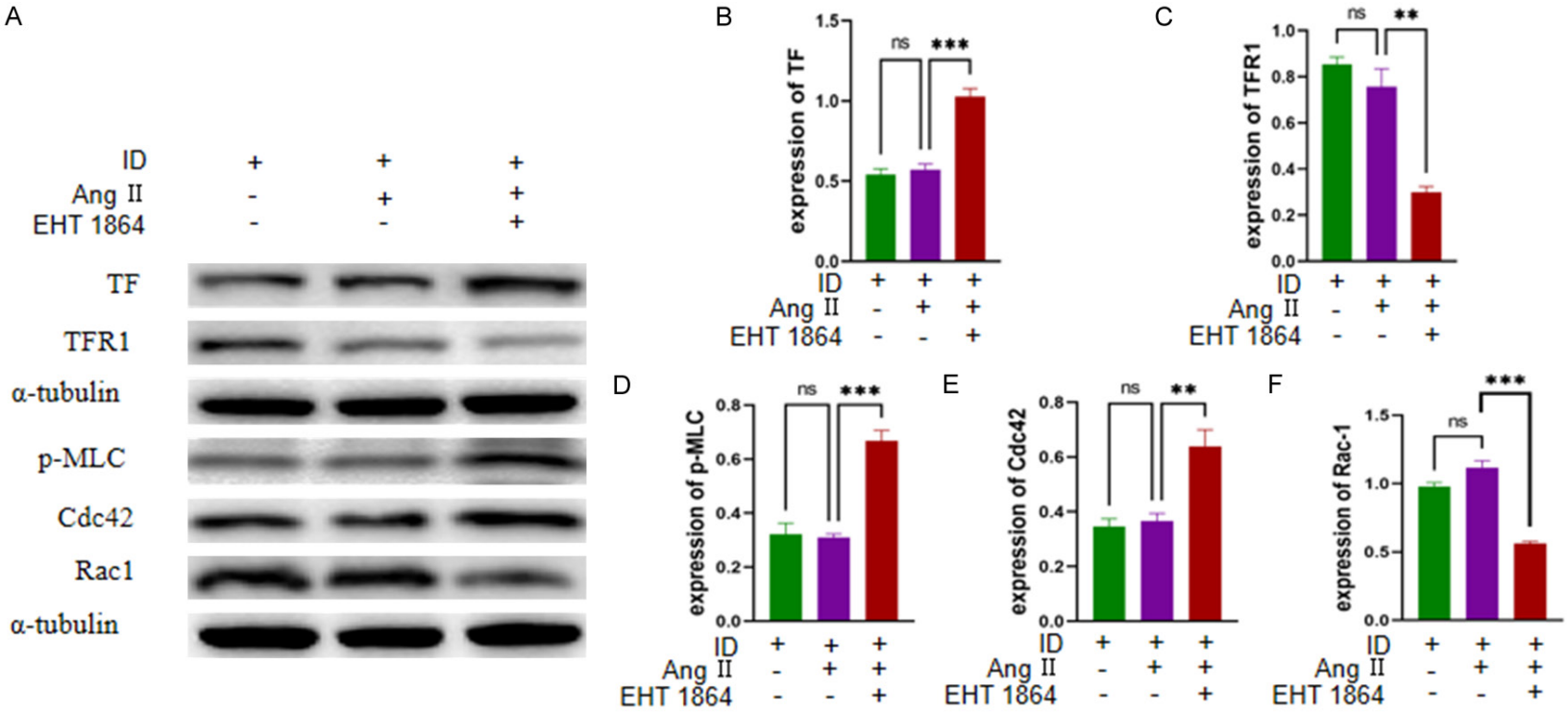

Figure 6. Inhibiting Rac1 alleviates iron metabolism disorders and improves VSMC dysfunction. Application of the Rac1 inhibitor EHT1864 decreased the expression of Rac1 and TFR1, whereas it increased the expression of TF, p-MLC and Cdc42 (A-F). Values are presented as the mean ± SD. **P < 0.01, ***P < 0.001. VSMCs, vascular smooth muscle cells; TFR1, transferrin receptor 1.

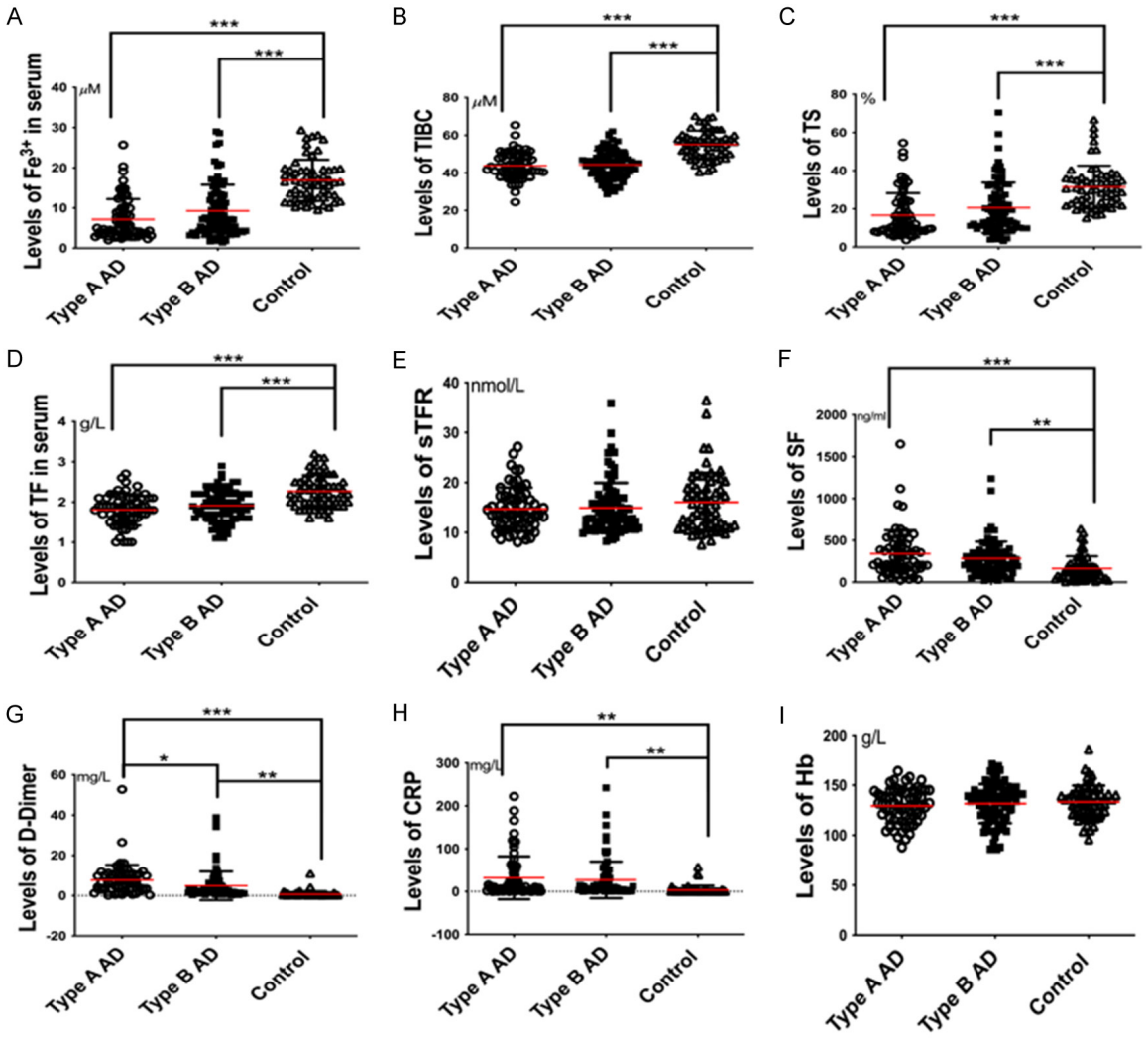

Figure 7. Patients with aortic diseases were iron deficient without anemia. The serum iron ion concentration (A), total iron binding capacity (B), transferrin saturation (C), and transferrin were significantly lower in AD patients compared with control patients (D). No significant differences were observed in soluble transferrin receptor, while the levels of ferritin were significantly increased in the serum of patients with AD compared to patients with hypertension (E, F). Serum D-dimmer and CRP concentrations in AD patients were higher than those in hypertensive patients (G, H). There was no significant difference in Hb concentrations among the groups (I). N type A AD = 66, N type B AD = 84, and N control = 60. Values are presented as the mean ± SD. $*P < 0.05$, $**P < 0.01$, $***P < 0.001$. AD, aortic dissection; CRP, C-reactive protein.

structural support and preserving cellular morphology and motility. An intact cytoskeletal framework constitutes the foundation for sustaining cellular functionality and actively participates in diverse physiological and pathological cellular processes [34]. F-actin is one of the major proteins that maintain the cytoskeleton, and the degree of cell-cell and cell-extracellular matrix adhesion is an important factor affecting the cytoskeleton and its functions. Animal experiments have validated the role of ID in modulating the expression of cytoskeletal proteins in VSMCs. Our findings indicate that ID has the potential to promote the formation of AMD in hypertensive mice by disrupting the structural integrity of the vessel wall. Consequently, our experimental results strongly suggest that ID may contribute to the development of AMD by inducing alterations in the skeletal structure and functional attributes of VSMCs.

To further investigate the effect of ID on VSMCs cytoskeleton and contractile function, we conducted in vitro cellular experiments. In addition

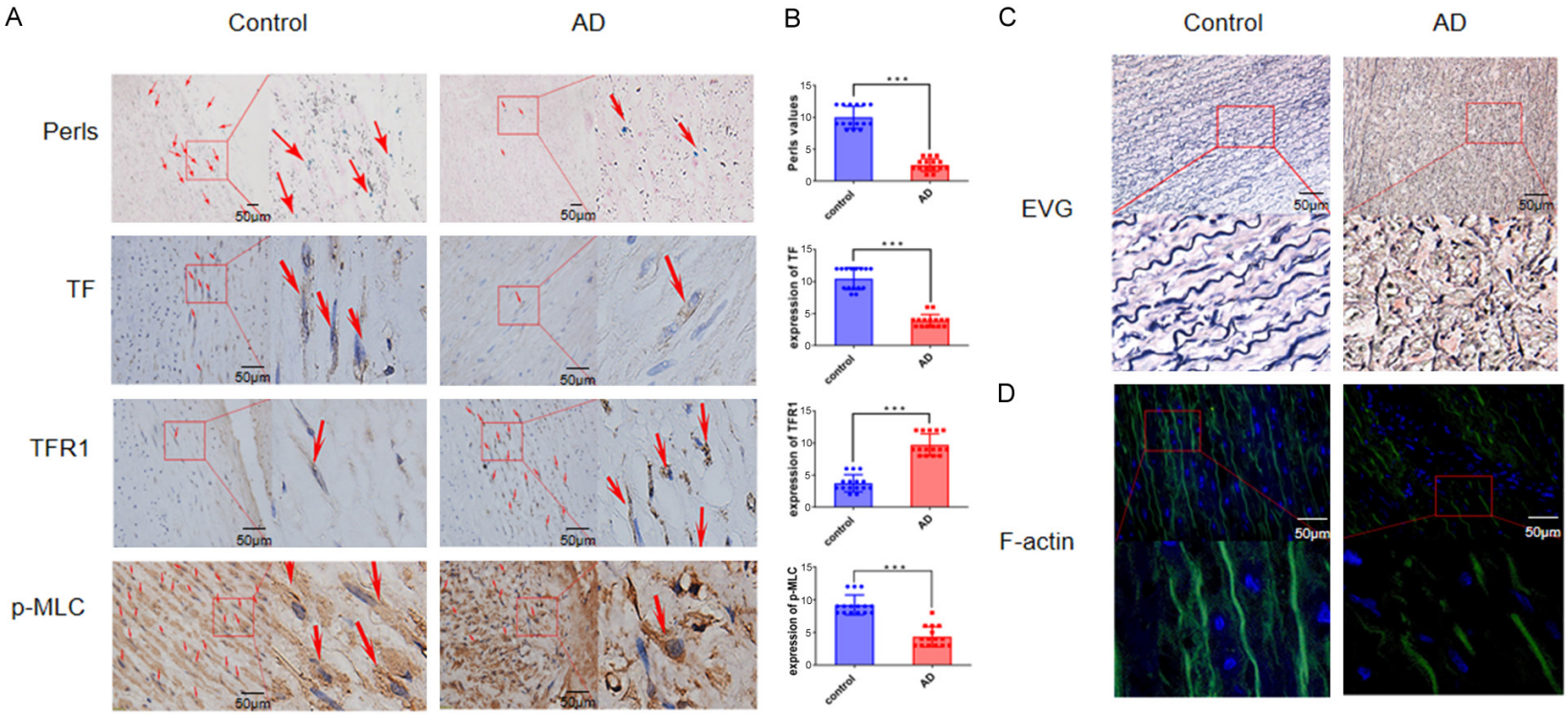

Figure 8. Comparison of aortic iron metabolism and wall structure between AD and control patients (N = 15). Prussian blue staining demonstrated reduced iron deposition in the middle layer of the AD aorta compared with the control group (A, B). IHC indicated downregulation of TF and upregulation of TFR1 in AD specimens (A, B). EVG staining showed that disintegrated and broken elastic fiber (black) and collagen deposition (red) were increased in AD specimens (C). The expression of F-actin protein (D) and p-MLC (A, B) was significantly lower in AD specimens compared to normal aortic specimens. Values are presented as the mean ± SD. ***P < 0.001. AD, aortic dissection; TF, transferrin; TFR1, transferrin receptor 1; IHC, Immunohistochemistry; EVG, Elastic van Gieson; p-MLC, phosphorylated myosin light chain.

to assessing F-actin levels, we also examined the expression of contractile function protein p-MLC and the Cdc42/Rac1 pathway protein in VSMCs. The p-MLC proteins facilitate contraction of vascular endothelial cells, while Cdc42 and Rac1, small G-proteins of the Rac family with GTPase activity, are key factors in regulating processes such as the cell cycle, cell migration, and actin remodeling within the cytoskeleton [35]. These molecules play critical roles in maintaining cytoskeletal integrity and function. Our findings revealed that under the ID condition, HASMCs exhibited morphological swelling. Furthermore, F-actin expression decreased, resulting in uneven distribution and aggregation of myofilaments towards the cell periphery. In our current investigation, we observed that in addition to diminishing F-actin levels, ID led to a reduction in the expression of p-MLC and Cdc42, while simultaneously increasing the expression of Rac1 both in vivo and in vitro. Following the application of EHT-1864, the expression of TFR1 and Rac1 decreased, whereas the expression of TF, p-MLC and Cdc42 increased. The results suggest that the utilization of EHT1864 effectively mitigated Ang II-induced cytoskeletal disruption and ameliorated dysregulation in iron metabolism.

Our analysis of clinical patient characteristics reveals that AD patients had higher systolic blood pressure, body mass index, and a greater incidence of ultrasound-detected liver damage, but a lower prevalence of diabetes compared to the control group. Acting as an acute phase reactant, the role of ferritin in iron homeostasis in the context of inflammation has a great importance in body protection against infection, injury, and cancer [36]. Our results showed that serum ferritin levels were higher in AD patients than those with hypertension, this indicates that AD patients are in a state of disease associated with multiple factors. Notably, patients with AD or aortic aneurysm (AA) demonstrated ID without anemia [37], attributable to the body's prioritization of hemoglobin production using iron ions; ID anemia occurs when body's iron stores become depleted [38]. Furthermore, our investigation revealed diminished iron deposition and reduced TF expression in the media of AD tissue specimens compared to normal aortic tissue. These findings collectively indicate the presence of ID in both the circulating blood and the aortic wall of AD patients.

In conclusion, our findings demonstrate that ID has the potential to facilitate the development of AMD in hypertensive situation and we first proposed that this detrimental effect is mediated through the disruption of the cytoskeleton of VSMCs via the Cdc42/Rac1 pathway. Our findings underscore the importance of maintaining iron metabolism homeostasis as a novel preventive approach for AD in hypertensive patients.

The study design has some areas that can be improved. We did not delve into the specific mechanism through which ID affects the cytoskeletal disorders of VSMCs via the Cdc42/Rac1 pathway, leading to the formation of AMD. To address this gap, future studies could use mouse models with Cdc42 smooth muscle cell-specific knockout.

Acknowledgements

The authors would like to thank all the patients and donors involved for providing tissue samples, and the Ethics Committee of Renmin Hospital of Wuhan University for supporting this study. These studies were supported by National Natural Science Foundation of China (82200522) and Central Universities Basic Research Project (2042021kf0136).

Disclosure of conflict of interest

None.

Address correspondence to: Ting Li, Department of Skin Medical Cosmetology, Renmin Hospital of Wuhan University, Wuhan 430060, Hubei, China. E-mail: liting1102@whu.edu.cn; Bowen Li, Department of Cardiovascular Surgery, Renmin Hospital of Wuhan University, Wuhan 430060, Hubei, China. E-mail: bowenli@whu.edu.cn

References

[1] Suzuki Y, Kaneko H, Yano Y, Okada A, Itoh H, Ueno K, Matsuoka S, Fujiu K, Michihata N, Jo T, Takeda N, Morita H, Yokota I, Node K, Yasunaga H and Komuro I. Dose-dependent relationship of blood pressure and glycaemic status with risk of aortic dissection and aneurysm. Eur J Prev Cardiol 2022; 29: 2338-2346.

[2] Hibino M, Otaki Y, Kobeissi E, Pan H, Hibino H, Taddese H, Majeed A, Verma S, Konta T, Yamagata K, Fujimoto S, Tsuruya K, Narita I, Kasahara M, Shibagaki Y, Iseki K, Moriyama T, Kondo M, Asahi K, Watanabe T, Watanabe T, Watanabe M and Aune D. Blood pressure, hypertension, and the risk of aortic dissection incidence and mortality: results from the J-SCH study, the UK Biobank study, and a meta-analysis of cohort studies. Circulation 2022; 145: 633-644.

[3] Liu X, Chen W, Zhu G, Yang H, Li W, Luo M, Shu C and Zhou Z. Single-cell RNA sequencing identifies an Il1rn+/Trem1+ macrophage subpopulation as a cellular target for mitigating the progression of thoracic aortic aneurysm and dissection. Cell Discov 2022; 8: 11.

[4] Li B, Wang Z, Hu Z, Zhang M, Ren Z, Zhou Z, Huang J and Hu X. P38 MAPK signaling pathway mediates angiotensin II-induced miR143/145 gene cluster downregulation during aortic dissection formation. Ann Vasc Surg 2017; 40: 262-273.

[5] Gammella E, Correnti M, Cairo G and Recalcati S. Iron availability in tissue microenvironment: the key role of ferroportin. Int J Mol Sci 2021; 22: 2986.

[6] Wang Y, Gao P, Li F and Du J. Insights on aortic aneurysm and dissection: role of the extracellular environment in vascular homeostasis. J Mol Cell Cardiol 2022; 171: 90-101.

[7] Lal A. Iron in health and disease: an update. Indian J Pediatr 2020; 87: 58-65.

[8] Sevimli G, Alston AE, Funk F, Flühmann B, Malli R, Graier WF and Eroglu E. Probing subcellular iron availability with genetically encoded nitric oxide biosensors. Biosensors (Basel) 2022; 12: 903.

[9] Beaufay F, Quarles E, Franz A, Katamanin O, Wholey WY and Jakob U. Polyphosphate functions in vivo as an iron chelator and fenton reaction inhibitor. mBio 2020; 11: e01017-20.

[10] Savarese G, von Haehling S, Butler J, Cleland JGF, Ponikowski P and Anker SD. Iron deficiency and cardiovascular disease. Eur Heart J 2023; 44: 14-27.

[11] Papalia F, Jouhra F, Amin-Youssef G, Shah AM, Charles-Edwards G and Okonko DO. Cardiac energetics in patients with chronic heart failure and iron deficiency: an in-vivo 31 P magnetic resonance spectroscopy study. Eur J Heart Fail 2022; 24: 716-723.

[12] Niwa K. Aortic dilatation in complex congenital heart disease. Cardiovasc Diagn Ther 2018; 8: 725-738.

[13] Mordi IR, Tee A and Lang CC. Iron therapy in heart failure: ready for primetime? Card Fail Rev 2018; 4: 28-32.

[14] Marques VB, Leal MAS, Mageski JGA, Fidelis HG, Nogueira BV, Vasquez EC, Meyrelles SDS, Simões MR and Dos Santos L. Chronic iron overload intensifies atherosclerosis in apolipoprotein E deficient mice: role of oxidative stress and endothelial dysfunction. Life Sci 2019; 233: 116702.

[15] Sawada H, Hao H, Naito Y, Oboshi M, Hirotani S, Mitsuno M, Miyamoto Y, Hirota S and Masuyama T. Aortic iron overload with oxidative stress and inflammation in human and murine abdominal aortic aneurysm. Arterioscler Thromb Vasc Biol 2015; 35: 1507-14.

[16] Martinez-Pinna R, Lindholt JS, Madrigal-Matute J, Blanco-Colio LM, Esteban-Salan M, Torres-Fonseca MM, Lefebvre T, Delbosc S, Laustsen J, Driss F, Vega de Ceniga M, Gouya L, Weiss G, Egido J, Meilhac O, Michel JB and Martin-Ventura J. From tissue iron retention to low systemic haemoglobin levels, new pathophysiological biomarkers of human abdominal aortic aneurysm. Thromb Haemost 2014; 112: 87-95.

[17] Moxon JV, Jones RE, Norman PE, Clancy P, Flicker L, Almeida OP, Hankey GJ, Yeap BB and Golledge J. Plasma ferritin concentrations are not associated with abdominal aortic aneurysm diagnosis, size or growth. Atherosclerosis 2016; 251: 19-24.

[18] Li B, Wang Z, Hong J, Che Y, Chen R, Hu Z, Hu X, Wu Q, Hu J and Zhang M. Iron deficiency promotes aortic medial degeneration via destructing cytoskeleton of vascular smooth muscle cells. Clin Transl Med 2021; 11: e276.

[19] Li Y, Pan Y, Wu X, Li Y, Wang H, Zhu H and Jiang L. Dual-modality imaging of atherosclerotic plaques using ultrasmall superparamagnetic iron oxide labeled with rhodamine. Nanomedicine (Lond) 2019; 14: 1935-1944.

[20] Baskin DG and Hewitt SM. Improving the state of the science of immunohistochemistry: the Histochemical Society's standards of practice. J Histochem Cytochem 2014; 62: 691-2.

[21] Zheng H, Li X, Zeng X, Huang C, Ma M, Lv X, Zhang Y, Sun L, Wang G, Du Y and Guan Y. TMEM16A inhibits angiotensin II-induced basilar artery smooth muscle cell migration in a WNK1-dependent manner. Acta Pharm Sin B 2021; 11: 3994-4007.

[22] Li G, Wang M, Caulk AW, Cilfone NA, Gujja S, Qin L, Chen PY, Chen Z, Yousef S, Jiao Y, He C, Jiang B, Korneva A, Bersi MR, Wang G, Liu X, Mehta S, Geirsson A, Gulcher JR, Chittenden TW, Simons M, Humphrey JD and Tellides G. Chronic mTOR activation induces a degradative smooth muscle cell phenotype. J Clin Invest 2020; 130: 1233-1251.

[23] Zhu Y, Lingala B, Baiocchi M, Tao JJ, Toro Arana V, Khoo JW, Williams KM, Traboulsi AA, Ham-

mond HC, Lee AM, Hiesinger W, Boyd J, Oyer PE, Stinson EB, Reitz BA, Mitchell RS, Miller DC, Fischbein MP and Woo YJ. Type A aortic dissection-experience over 5 decades: JACC historical breakthroughs in perspective. J Am Coll Cardiol 2020; 76: 1703-1713.

[24] Li F, Wang S, Gao Q, Chen X, Yin G, Yu C, Wang Y, Wang X, Qiao E, Meddings Z, Wang W, Zhao S and Teng Z. Vessel structural stress mediates aortic media degeneration in bicuspid aortopathy: new insights based on patient-specific fluid-structure interaction analysis. J Biomech 2021; 129: 110805.

[25] Whelton PK, Carey RM, Aronow WS, Casey DE Jr, Collins KJ, Dennison Himmelfarb C, DePalma SM, Gidding S, Jamerson KA, Jones DW, MacLaughlin EJ, Muntner P, Ovbiagele B, Smith SC Jr, Spencer CC, Stafford RS, Taler SJ, Thomas RJ, Williams KA Sr, Williamson JD and Wright JT Jr. 2017 ACC/AHA/AAPA/ABC/ACPM/AGS/APhA/ASH/ASPC/NMA/PCNA guideline for the prevention, detection, evaluation, and management of high blood pressure in adults: a report of the American College of Cardiology/American Heart Association Task Force on clinical practice guidelines. Hypertension 2018; 71: e13-e115.

[26] Gaddum NR, Keehn L, Guilcher A, Gomez A, Brett S, Beerbaum P, Schaeffter T and Chowienczyk P. Altered dependence of aortic pulse wave velocity on transmural pressure in hypertension revealing structural change in the aortic wall. Hypertension 2015; 65: 362-9.

[27] Shi F, Wang Z, Wu Q, Zhong X, Zhang M, Li B, Ren W, Yuan S and Chen Y. Iron deficiency promotes aortic media degeneration by activating endoplasmic reticulum stress-mediated IRE1 signaling pathway. Pharmacol Res 2022; 183: 106366.

[28] Miano JM, Fisher EA and Majesky MW. Fate and state of vascular smooth muscle cells in atherosclerosis. Circulation 2021; 143: 2110-2116.

[29] Zhang F, Guo X, Xia Y and Mao L. An update on the phenotypic switching of vascular smooth muscle cells in the pathogenesis of atherosclerosis. Cell Mol Life Sci 2021; 79: 6.

[30] Sorokin V, Vickneson K, Kofidis T, Woo CC, Lin XY, Foo R and Shanahan CM. Role of vascular smooth muscle cell plasticity and interactions in vessel wall inflammation. Front Immunol 2020; 11: 599415.

[31] Lampugnani MG, Dejana E and Giampietro C. Vascular endothelial (VE)-cadherin, endothelial adherens junctions, and vascular disease. Cold Spring Harb Perspect Biol 2018; 10: a029322.

[32] Rho SS, Ando K and Fukuhara S. Dynamic regulation of vascular permeability by vascular endothelial cadherin-mediated endothelial cell-cell junctions. J Nippon Med Sch 2017; 84: 148-159.

[33] Albini PT, Segura AM, Liu G, Minard CG, Coselli JS, Milewicz DM, Shen YH and LeMaire SA. Advanced atherosclerosis is associated with increased medial degeneration in sporadic ascending aortic aneurysms. Atherosclerosis 2014; 232: 361-8.

[34] Rajan S, Yoon J, Wu H, Srapyan S, Baskar R, Ahmed G, Yang T, Grintsevich EE, Reisler E and Terman JR. Disassembly of bundled F-actin and cellular remodeling via an interplay of Mical, cofilin, and F-actin crosslinkers. Proc Natl Acad Sci U S A 2023; 120: e2309955120.

[35] Yu D, Makkar G, Strickland DK, Blanpied TA, Stumpo DJ, Blackshear PJ, Sarkar R and Monahan TS. Myristoylated alanine-rich protein kinase substrate (MARCKS) regulates small GTPase Rac1 and Cdc42 activity and is a critical mediator of vascular smooth muscle cell migration in intimal hyperplasia formation. J Am Heart Assoc 2015; 4: e002255.

[36] Mahroum N, Alghory A, Kiyak Z, Alwani A, Seida R, Alrais M and Shoenfeld Y. Ferritin - from iron, through inflammation and autoimmunity, to COVID-19. J Autoimmun 2022; 126: 102778.

[37] Kumar A, Sharma E, Marley A, Samaan MA and Brookes MJ. Iron deficiency anaemia: pathophysiology, assessment, practical management. BMJ Open Gastroenterol 2022; 9: e000759.

[38] Sun K, Guo Z, Hou L, Xu J, Du T, Xu T and Guo F. Iron homeostasis in arthropathies: from pathogenesis to therapeutic potential. Ageing Res Rev 2021; 72: 101481.